



# Unified hardening (UH) model for unsaturated expansive clays

Yangping Yao<sup>1</sup> · Yichuan Tian<sup>1</sup> · Wenjie Cui<sup>1</sup> · Ting Luo<sup>1</sup> · Shanshan Li<sup>1</sup>

Received: 6 February 2023 / Accepted: 2 November 2023 / Published online: 16 December 2023  
 © The Author(s), under exclusive licence to Springer-Verlag GmbH Germany, part of Springer Nature 2023

## Abstract

In this paper, by introducing a new yielding mechanism based on the widely acknowledged double-structure theory, the original UH model for unsaturated soils is extended to capture the behaviour of expansive clays. A novel expansion potential is further established to evaluate the effect of overconsolidation on the volume change of unsaturated expansive clays during wetting. With only one additional parameter, the proposed model can describe the behaviour of both wetting-collapse and wetting-induced swelling for unsaturated clays. Comparisons between model predictions and test results show a good agreement which verifies the capability of the proposed model in charactering the features of unsaturated expansive clays under various stress histories and stress paths.

**Keywords** Constitutive relation · Elastoplasticity · Expansive clays · Suction · Unsaturated clays

## List of symbols

$D_{ijkl}^{ep}$	Elasto-plastic constitutive tensor	$\tilde{p}$	Mean net stress in transformed stress space
$E$	Elastic modulus	$\bar{p}$	Reference mean effective stress in transformed stress space
$f$	Current yield function	$p_{at}$	Atmospheric pressure
$\bar{f}$	Reference yield surface	$p^c$	Reference suction stress
$\tilde{f}$	Current yield surface in the transformed stress space	$p_s$	Suction stress
$f_d$	Magnification factor	$p_x$	Right intersection of current yield surface and p-axis
$G$	Shear modulus	$\bar{p}_x$	Right intersection of reference yield surface and p-axis
$H$	Unified hardening parameter	$p_x^*$	Preconsolidation pressures for saturated clays
$J$	Material parameter representing the swelling capacity of expansive clays	$\bar{p}_x^*$	Right intersection of the reference yield surface and the p axis for saturated clays
$K$	Elastic bulk modulus	$\bar{p}_{x0}$	Right intersection of reference yield surface and p-axis in the initial condition
$k$	A constant describing the increase in cohesion with suction	$q$	Deviatoric stress
$K_m$	Scale factor for determinate macrostructural plastic volumetric strain	$\hat{q}$	Deviatoric stress considering the suction
$L$	Lame's constant	$\bar{q}$	Reference deviatoric stress
$M$	Characteristic state stress ratio	$\tilde{q}$	Deviatoric stress in transformed stress space
$M_{Ys}$	Potential failure stress ratio	$\hat{q}_c$	Deviatoric stress under triaxial compression condition in the SMP criterion
$\tilde{M}_{Ys}$	Potential failure stress ratio in transformed stress space	$R_s$	Overconsolidation parameter
$p$	Net mean stress	$\tilde{R}_s$	Overconsolidation parameter in transformed stress space
$\hat{p}$	Mean stress considering the suction	$s_0$	Maximum suction in history
$\bar{p}$	Reference mean effective stress	$X_m$	Scale factor for determinate microstructural volumetric strain
		$\beta$	Material parameter controlling the rate of increase of soil stiffness with suction

✉ Wenjie Cui  
 wcui21@buaa.edu.cn

<sup>1</sup> School of Transportation Science and Engineering, Beihang University, Beijing 100191, China

$\gamma$	Material parameter defining the maximum soil stiffness
$\delta_{ij}$	Kronecker's delta
$\varepsilon_d$	Total deviatoric strain
$\varepsilon_d^e$	Elastic deviatoric strain
$\varepsilon_d^p$	Plastic deviatoric strain
$\varepsilon_{klp_m}^p$	Plastic strain induced by the microstructural deformation
$\varepsilon_{klp_s}^e$	Elastic strain induced by $p_s$
$\varepsilon_m$	Microstructural volumetric strain
$\varepsilon_v$	Total volumetric strain
$\varepsilon_v^e$	Elastic volumetric strain
$\varepsilon_{vp}^e$	Elastic volumetric strain induced by the change of the net stress
$\varepsilon_{vp}^p$	Plastic volumetric strain induced by the expansion of the current LC yield surface
$\varepsilon_{vs}$	Volumetric strain induced by the suction change
$\varepsilon_{vs}^e$	Elastic volumetric strain induced by the suction change
$\varepsilon_{vs}^p$	Macrostructural plastic volumetric strain induced by suction change
$\widehat{\eta}$	Stress ratio
$\widetilde{\eta}$	Stress ratio in transformed stress space
$\widehat{\theta}$	Lode's angel
$\kappa$	Slope of unloading line for unsaturated clays
$\kappa_s$	Slope of compression line in the $e - \ln s$ plane when the suction is less than or equal to $s_0$
$\Lambda$	Plastic multiplier
$\lambda(0)$	Slope of the compression curves for saturated clays
$\lambda(s)$	Slope of the compression curves for unsaturated clays with the suction $s$
$\lambda_s$	Slope of compression line in the $e - \ln s$ plane when the suction exceeds $s_0$
$\nu$	Poisson's ratio
$\rho_d$	Initial dry density
$\rho_w$	Density of water
$\sigma_i$	Principal stress
$\widehat{\sigma}_i$	Principal stress considering the suction
$\sigma_{ij}$	Stress tensor
$\widehat{\sigma}_{ij}$	Stress tensor considering the suction
$\widetilde{\sigma}_{ij}$	Transformed stress tensor
$\sigma_{ij}^{p_s}$	Stress related to $p_s$
$\sigma_v$	Vertical pressures
$\widehat{\Omega}$	Coefficient related to overconsolidation
$\widetilde{\Omega}$	Coefficient related to overconsolidation in transformed stress space

## 1 Introduction

Expansive clays under unsaturated status usually exhibit the characteristics of volume increase and strength reduction during wetting due to the mechanical and physico-chemical phenomena occurring at particle level which are a consequence of the particular properties of the active clay minerals [9, 12]. These features, if not adequately considered in the associated practical design, may induce nonuniform foundation settlement and further result in structural damage to the overlaying infrastructures. Therefore, it is of great significance to investigate the behaviour of unsaturated expansive clays and to develop the relevant modelling tools.

With the advances in testing techniques and apparatus, a number of experimental studies have been carried out to study the mechanical behaviour of expansive clays [6, 8, 10, 22]. Based on these findings from the experimental studies, it has been widely acknowledged that the special features of unsaturated expansive clays are attributed to their special structure which involves two distinct pore systems, i.e. the macrostructure associated with the large-scale material structure and the microstructure accounting for the active clay minerals [23]. To capture the behaviour of expansive clays, a pioneering elasto-plastic constitutive framework was established by Gens and Alonso [9] which was an extension of the Basic Barcelona Model (BBM) [1] for typical unsaturated soils by taking into account of the effect of the microstructure in addition to that of the macrostructure. Within this framework, Alonso et al. [3] further proposed the Barcelona Expansive Model (BExM) for unsaturated expansive clays, in which the characteristics of volume increase during wetting were modelled by considering the interaction of the double structures, i.e. the swelling of microstructure can lead to the plastic expansion of the macrostructure. By combining the theory of double structures with the generalized plasticity theory, a constitutive model has been established by Sanchez et al. [23] to describe the deformation characteristics of unsaturated expansive clays. Mašín [19] introduced hydraulic coupling into the double structures, in which the influence of hydraulic action on the unsaturated expansive clays was taken into account. Wang et al. [29] verified the capability of BExM in reproducing the main features of swelling pressure development and microstructural volume change of unsaturated expansive soils during wetting, and further analysed the limitations of the double structure theory. A constitutive model was established by Wang et al. [31] by introducing the concept of the critical saturation state, which was demonstrated to be able to well describe the volumetric behaviour of compacted bentonite. Kyokawa [12] proposed a hydro-

mechano-chemical model for unsaturated expansive soils within the double structure framework, which was shown to be capable of describing the macroscale soil skeleton behaviour and the nanoscale interlaminar behaviour of mineral crystals based on the surface phenomena. Lu et al. [17] proposed a coupled chemo-hydro-mechanical model for compacted bentonite based on the BExM by introducing the osmotic stress, which was shown to be able to capture the main features of the volumetric change behaviour in the coupled chemo-hydro-mechanical processes. Another approach for modelling the constitutive behaviour of unsaturated expansive clays is to follow a similar manner to that adopted for typical unsaturated soils which only takes into account the volume change at the macroscopic level [5, 14, 16, 21, 24–26, 32, 49]. Sun and Sun [27] proposed a modelling approach for expansive soils by introducing the equivalent void ratio curve (EVRC) into an existing hydro-mechanical model for unsaturated soils. The hydro-mechanical coupling in the expansive soils, i.e. the effect of saturation on the stress–strain relationship and the effect of volume change on the water-retention behaviour, could be well captured. On the basis of thermodynamic theory, Li et al. [13] presented the formulation of work input that was suitable for unsaturated expansive clays and further developed a constitutive model to describe the swelling characteristics for expansive clays with four groups of work-conjugate variables. These constitutive models have been shown to be capable of predicting the stress–strain relationship of normally consolidated unsaturated expansive clays. However, most of them have not specifically accounted for the influence of the overconsolidation ratio (OCR) on wetting volume change, which may lead to inaccurate predicted results when they were applied to model the behaviour of heavily overconsolidated unsaturated expansive clays. To adequately describe the behaviour of unsaturated expansive clays with a wide range of OCRs, it is necessary to establish the constitutive relation based on an existing powerful and robust framework for heavily overconsolidated unsaturated clays.

By introducing an innovative hardening parameter  $H$  into the modified Cam-clay model, Yao et al. [36] proposed the unified hardening (UH) model for overconsolidated clays, which can simulate many characteristics of overconsolidated clays such as shear dilatation and strain softening. When modelling the normally consolidated clays, the UH model can reduce to the modified Cam-clay model. Based on the same constitutive framework, a series of advanced UH models considering the effects of various complex conditions such as temperature variation, partial saturation, and anisotropy have been developed [37, 38, 40, 43, 44]. In this paper, the framework of the UH model for overconsolidated unsaturated soils [41] is selected as the basis.

While inheriting the advantages of the original UH model for unsaturated soils [41] in describing the features of overconsolidated unsaturated soils, a novel constitutive relation for unsaturated expansive clays is proposed by introducing a new yield surface, which can be used to measure the plastic swelling strain of expansive clays during wetting, and an expansion potential, which is established based on the interaction mechanism of the double structures theory. The proposed model is demonstrated to be capable of capturing the effects of both OCR and initial dry density on the swelling characteristics of expansive clays. Compared with the UH model for unsaturated soils, the new model, referred to as the UH model for unsaturated expansive clays, requires only one new additional parameter. Its capability in describing the volume change of overconsolidated unsaturated expansive clays during wetting is validated by the comparison against existing test data in the literature. It is noted that this paper adopts a compression positive sign convention.

## 2 Review of UH model for unsaturated clays

Yao et al. [36] proposed the UH model for overconsolidated clays, in which the characteristics of strain hardening and softening, shear contraction and dilatation were described by introducing a novel hardening parameter. Based on the same framework, the UH model for unsaturated soils was further developed [41], where the current yield surface and the reference yield surface were used to capture the stress–strain relation of overconsolidated unsaturated soils as shown in Fig. 1. The current yield surface can be expressed as

$$f = \ln(p + p_s) + \ln \left[ 1 + \frac{q^2}{M^2(p + p_s)^2} \right] - \ln(p_x + p_s) = 0 \quad (1)$$

where  $p$  is the net mean stress of the current stress point,  $p_s = ks$  is the suction stress, which has the same definition as that in BBM [1] and represents the contribution of suction to soil cohesion, and  $p_x$  is the mean net stress at the right intersection of current yield surface and  $p$ -axis under a known suction  $s$ , as shown in Fig. 2. The reference yield surface can be expressed as

$$\bar{f} = \ln(\bar{p} + p_s) + \ln \left[ 1 + \frac{\bar{q}^2}{M^2(\bar{p} + p_s)^2} \right] - \ln(\bar{p}_x + p_s) = 0 \quad (2)$$

where  $\bar{p}$  and  $\bar{q}$  are the reference mean effective stress and reference deviatoric stress, respectively, and  $\bar{p}_x$  is the mean net stress at the right intersection of reference yield surface

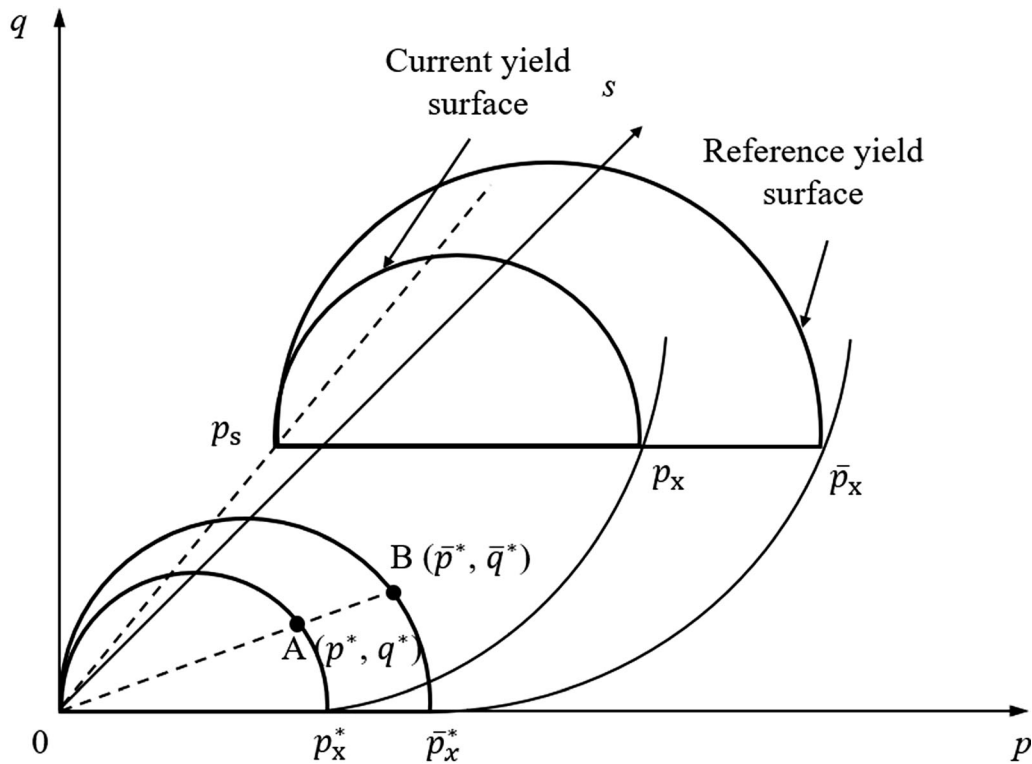


Fig. 1 The current yield surface and the reference yield surface in  $p$ – $q$ – $s$  space

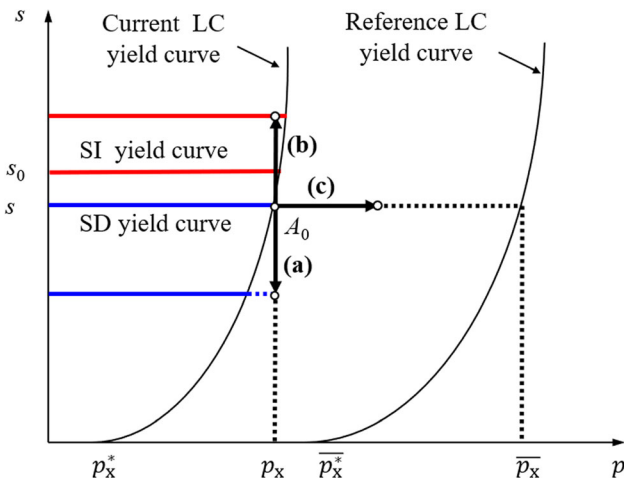


Fig. 2 Yield surfaces in  $p$ – $s$  plane and its evolution

and  $p$ -axis under an unsaturated condition with a known suction  $s$ , as shown in Fig. 2.

The UH model for unsaturated soils adopts the reference LC yield surface and the current LC yield surface to consider the influence of suction change on soil volume change. The current LC yield surface equation which was reported by Alonso et al. [1] can be written as

$$\frac{p_x}{p^c} = \left( \frac{p_x^*}{p^c} \right)^{\frac{\lambda(0)-\kappa}{\lambda(s)-\kappa}} \tag{3}$$

where

$$\lambda(s) = \lambda(0)[(1 - \gamma)\exp(-\beta s) + \gamma] \tag{4}$$

where  $p_x^*$  is the preconsolidation pressures for saturated clays,  $\lambda(0)$  and  $\lambda(s)$  are the slopes of the compression curves for saturated clays and unsaturated clays with the suction  $s$ , respectively,  $\kappa$  is the slope of unloading line for unsaturated clays,  $p^c$  is the reference suction stress and its definition is consistent with that in BBM, i.e. the change of suction can only induce the elastic strain when the net mean stress is equal to  $p^c$ ,  $\beta$  and  $\gamma$  are material parameters. The reference LC yield surface equation can be written as

$$\frac{\bar{p}_x}{p^c} = \left( \frac{\bar{p}_x^*}{p^c} \right)^{\frac{\lambda(0)-\kappa}{\lambda(s)-\kappa}} \tag{5}$$

where  $\bar{p}_x^*$  is the mean net stress at the right intersection of the reference yield surface and the  $p$  axis under fully saturated condition.

Although the original UH model for unsaturated soils is demonstrated to be capable of capturing the characteristics of typical unsaturated clays, it cannot adequately model the swelling behaviour of unsaturated expansive clays during wetting. Therefore, it is necessary to further extend the



model based on the investigation of the swelling mechanism of unsaturated expansive clays.

### 3 Swelling mechanism based on the double-structure theory

In BExM, Alonso et al. [3] believed that the swelling of expansive clays during wetting was related to its microstructure. When the suction of expansive clays decreases, the swelling of the clay microstructure can induce irreversible expansive volume change of the macrostructure. As shown in Fig. 3, before wetting, the microstructure in expansive soils is arranged densely and the macrostructural pores are relatively small. During wetting, as the microstructure swells, structural rearrangement of the soil skeleton occurs resulting in the overall expansion of the expansive soils [28]. As stated by Sanchez et al. [23], the expansive soil with a higher OCR is in a state of a denser packing of the material. Therefore, the microstructural swelling can significantly affect the global arrangement of clay aggregates and further leads to larger macrostructural plastic strains, which agrees with the features described by BExM [3] and was supported by the experiment by Ye et al. [45].

Following a similar approach to that adopted by the BExM [3], the SD yield surface is introduced to describe the expansive plastic volumetric change induced by microstructural expansion when suction decreases. Based on the experimental results of expansive soils, Lu et al. [18]

found that the yielding suctions during both wetting and drying under different net stresses were similar, indicating that the SI and SD yield surfaces were almost parallel to the  $p$ -axis in  $p$ - $s$  plane. For simplicity, the SD yield surface in this paper is assumed to be parallel to the  $p$ -axis, as shown in Fig. 2. When the suction of unsaturated expansive clays changes, the SD yield surface will move with the current suction. In this work, it is assumed that the SD yield surface is only active when the suction decreases such that the macrostructural expansive plastic volumetric strain induced by the microstructural swelling can be characterized. Meanwhile, the suction increase (SI) yield surface defined by the BBM [1] is adopted, which can be written as:

$$s = s_0 \quad (6)$$

where  $s_0$  is the maximum suction in history. When the stress status is within the plane enclosed by the SI and reference LC yield surfaces, suction increase can only result in elastic shrinkage. When the suction exceeds  $s_0$ , the SI yield surface will expand with increasing suction and irreversible contractive volumetric change is induced.

In summary, different stress paths in the  $p$ - $s$  plane requires the activation of the SD yield surface or the SI yield surface, resulting in different mechanisms of the volume change in the proposed model. When the unsaturated expansive clays experience wetting from an initial stress point  $A_0$  under a constant net mean stress, as shown by path (a) in Fig. 2, the suction decreases and the current stress point tends to move downward. Therefore, both the

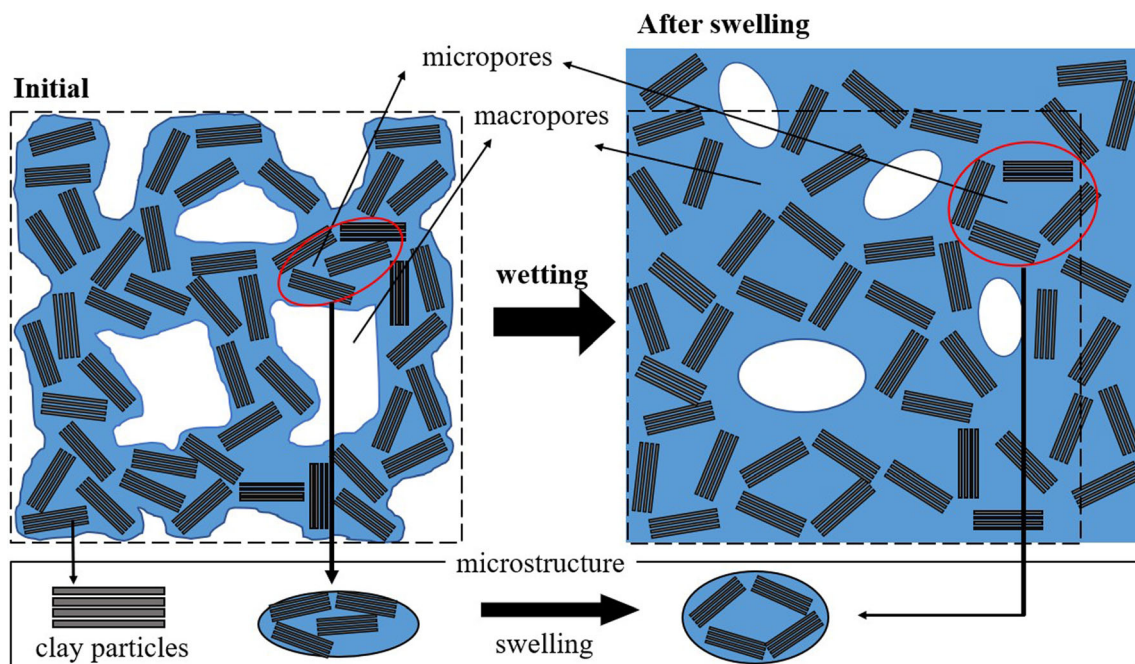


Fig. 3 Swelling mechanism of unsaturated expansive clays with double-structure during wetting

SD and current LC yield surfaces are activated, while the SI yield surface stays still. Under this circumstance, the volumetric change of unsaturated expansive clays is composed of three parts which can be expressed as:

$$d\varepsilon_v = d\varepsilon_{vs}^p + d\varepsilon_{vs}^e + d\varepsilon_{vp}^p \tag{7}$$

where  $d\varepsilon_{vs}^p$  is the plastic volumetric strain induced by the drift of the SD yield surface which is associated with the swelling of the microstructure,  $d\varepsilon_{vs}^e$  is the elastic volumetric strain induced by the suction decreasing, and  $d\varepsilon_{vp}^p$  is the plastic volumetric strain induced by the expansion of the current LC yield surface. Under the stress path of drying with a constant net mean stress (see path (b) in Fig. 2), although the SD yield surface and the current LC yield surface are updated with increasing suction, those mobilisations are assumed to not induce any plastic volumetric strain. Meanwhile, following the same mechanism defined by the original UH model for unsaturated clays, the SI yield surface is only activated once the suction exceeds the maximum suction in history  $s_0$ . Therefore, when  $s \leq s_0$ , the total volumetric strain of unsaturated expansive clays during drying is only composed of the elastic volumetric strain induced by the suction increase,  $d\varepsilon_{vs}^e$ . When  $s > s_0$ , the plastic volumetric strain induced by the activation of the SI yield surface,  $d\varepsilon_{vs}^p$ , should be introduced and the total volumetric strain can be expressed as

$$d\varepsilon_v = d\varepsilon_{vs}^p + d\varepsilon_{vs}^e \tag{8}$$

Under the stress path with a constant suction, as shown by path (c) in Fig. 2, the behaviour of the volumetric change for the proposed model is the same as that described by the original UH model for unsaturated soils.

## 4 Constitutive equations of UH model for unsaturated expansive clays

### 4.1 Expansion potential based on the double-structure theory

Following a similar approach to that in BExM [3], the macrostructural plastic volumetric strain,  $d\varepsilon_{vs}^p$ , could be expressed as a linear function of the microstructural volumetric strain, given as

$$d\varepsilon_{vs}^p = K_m d\varepsilon_m \tag{9}$$

where  $K_m$  is a scale factor and  $d\varepsilon_m$  is the microstructural volumetric strain. Gens and Alonso [9] believed that the microstructure was saturated in which only elastic volumetric strain could appear. Meanwhile, Lloret and Villar [15] and Wang et al. [28] found that the intra-aggregate pore volumes in expansive soils appeared to be

independent with the compaction effort. For simplicity, it is assumed in this paper that the microstructural volumetric change is only related to suction. Therefore, based on the swelling mechanism described above, during wetting, the swelling of the microstructure could be considered as a part of the elastic volumetric strain induced by the change of suction, expressed as

$$d\varepsilon_m = X_m d\varepsilon_{vs}^e \tag{10}$$

where  $X_m$  is a scale factor. Then  $X_m$  and  $K_m$  are considered as a factor  $f_d$ , the expansion potential describing the plastic volumetric strain during wetting can be expressed as

$$d\varepsilon_{vs}^p = f_d d\varepsilon_{vs}^e \tag{11}$$

where

$$d\varepsilon_{vs}^e = \frac{\kappa_s \cdot ds}{[(1 + e_0)(s + p_{at})]} \tag{12}$$

where  $\kappa_s$  is the slope of compression line in the  $e - \ln s$  plane when the suction is less than or equal to  $s_0$ ,  $p_{at}$  is the atmospheric pressure.  $f_d$  is the magnification factor. Existing studies [9, 15, 23, 46] revealed that both the dry density and OCR had a significant impact on the swelling pressure and the macrostructural volume change of expansive soils, respectively. Therefore,  $f_d$  is given as:

$$f_d = J^{\frac{\rho_d}{\rho_w}} (1 - R_s)^2 \tag{13}$$

where  $\rho_d$  is the initial dry density of the clays, which is the dry density of clays at the beginning of wetting representing the associated compaction status of the clays.  $\rho_w$  is the density of water, and  $J$  is a material parameter representing the swelling capacity of expansive clays, which can be obtained through the swelling pressure tests under a certain dry density. When  $J = 0$ , the macrostructural plastic volumetric strain  $d\varepsilon_{vs}^p = 0$ , and thus the model reduces to the UH model for unsaturated soils [41].  $R_s$  is a parameter associated with the overconsolidation ratio (OCR), which is the ratio of the stress at the current stress point to the stress at the reference stress point. After considering the influence of suction, it can be expressed as [41]

$$R_s = \frac{p + p_s}{\bar{p}_{x0} + p_s} = \frac{(p + p_s) \left( 1 + \frac{\hat{\eta}^2}{M^2} \right)}{\bar{p}_{x0} \exp \left( \frac{\lambda(0) - \kappa (e_{vp}^p + e_{vs}^e)}{\lambda(s) - \kappa} \right) + p_s} \tag{14}$$

where  $\bar{p}_{x0}$  is the initial reference preconsolidation pressure under unsaturated condition (the initial value of  $\bar{p}_x$ ) and  $\hat{\eta}$  is stress ratio defined as  $q/(p + p_s)$ . It should be noted that a lower value of  $R_s$  can lead to the more significant rearrangement of the clay minerals induced by the swelling of the microstructure during wetting, and thus induce a higher volume change of the macrostructure.

During drying, as the suction increases, although the SD yield surface updates, its mobilisation is assumed to not induce any plastic volumetric strain. Therefore,  $f_d$  can be expressed during drying as

$$f_d = 0 \quad (15)$$

When the suction exceeds the maximum suction in history  $s_0$ , the SI yield is activated and the relevant plastic volumetric strain induced by suction change,  $d\varepsilon_{vs}^p$ , can be expressed as

$$d\varepsilon_{vs}^p = \frac{\lambda_s - \kappa_s}{v} \frac{ds}{s + p_{at}} \quad (16)$$

where  $\lambda_s$  is the slope of compression line in the  $e - \ln s$  plane when the suction exceeds  $s_0$

## 4.2 Unified hardening parameter $H$

The hardening law can be expressed as

$$\frac{dp_x^*}{p_x^*} = \frac{1 + e_0}{\lambda(0) - \kappa} dH \quad (17)$$

where  $H$  is unified hardening parameter which is related to the plastic volumetric strain induced by the change of the net mean stress,  $d\varepsilon_{vp}^p$ , expressed as

$$dH = \frac{M_{Ys}^4 - \hat{\eta}^4}{M^4 - \hat{\eta}^4} d\varepsilon_{vp}^p \quad (18)$$

where  $M$  is characteristic state stress ratio and  $M_{Ys}$  is the potential failure stress ratio [39] given as

$$M_{Ys} = 6 \left[ \sqrt{\frac{\chi}{R_s} \left( 1 + \frac{\chi}{R_s} \right)} - \frac{\chi}{R_s} \right] \quad (19)$$

where

$$\chi = \frac{M^2}{12(3 - M)} \quad (20)$$

$$\hat{\eta} = \frac{\hat{q}}{\hat{p}} \quad (21)$$

$$\hat{p} = p + p_s \quad (22)$$

$$\hat{q} = q \quad (23)$$

## 4.3 Strain increments

In this model, the elastic volumetric strain can be expressed as:

$$d\varepsilon_v^e = d\varepsilon_{vp}^e + d\varepsilon_{vs}^e \quad (24)$$

It consists of two parts, the first part is the elastic volumetric strain induced by the change of the net stress,  $d\varepsilon_{vp}^e$ , which can be expressed as:

$$d\varepsilon_{vp}^e = \frac{dp}{K} \quad (25)$$

where

$$K = \frac{E}{3(1 - 2\nu)} \quad (26)$$

$$E = \frac{3(1 - 2\nu)(1 + e_0)}{\kappa} p \quad (27)$$

The second part is the elastic volumetric strain induced by the suction change,  $d\varepsilon_{vs}^e$ , given by Eq. (12).

The elastic deviatoric strain induced by the shear stress can be expressed as

$$d\varepsilon_d^e = \frac{dq}{3G} \quad (28)$$

where  $G$  is the shear modulus.

The plastic strain consists of two components. One part is the plastic strains induced by the net stress change, which are defined following the same manner as that in the UH model for unsaturated soils, given as

$$d\varepsilon_{vp}^p = \Lambda \frac{\partial f}{\partial \hat{p}} \quad (29)$$

$$d\varepsilon_d^p = \Lambda \frac{\partial f}{\partial \hat{q}} \quad (30)$$

where  $\Lambda$  is the plastic multiplier which can be derived from the consistency condition as:

$$\Lambda = \frac{c_p \hat{\Omega} \frac{\partial f}{\partial \hat{p}} d\hat{p} + \frac{\partial f}{\partial \hat{q}} d\hat{q} + f_s ds}{\frac{\partial f}{\partial \hat{p}}} \quad (31)$$

where

$$A_0 = \frac{p_x^*}{p_x + p_s} \frac{\lambda(0) - \kappa}{\lambda(s) - \kappa} \left( \frac{p_x^*}{p^c} \right)^{\frac{\lambda(0) - \lambda(s)}{\lambda(s) - \kappa}} \quad (32)$$

$$f_s = -\frac{1}{p_x + p_s} \left( k + \frac{\partial p_x}{\partial \lambda(s)} \frac{\partial \lambda(s)}{\partial s} \right) \quad (33)$$

$$p_x^* = p^c \left( \frac{p_x}{p^c} \right)^{\frac{\lambda(s) - \kappa}{\lambda(0) - \kappa}} \quad (34)$$

$$p_x = p + \frac{q^2}{M^2 \hat{p}} \quad (35)$$

$$\hat{\Omega} = \frac{M^4 - \hat{\eta}^4}{M_{Ys}^4 - \hat{\eta}^4} \quad (36)$$

$$c_p = \frac{\lambda(0) - \kappa}{1 + e_0} \quad (37)$$

while the plastic volumetric strains induced by suction change are defined by Eqs. (11) and (16). When yielding occurs on both LC and SD, the total plastic strain can be obtained by the plastic strains induced by the activation of each yield surface.

The associated flow rule is adopted by the proposed model.

#### 4.4 Elastoplastic stress–strain relation under triaxial stress state

Combining the above constitutive equations, the total volumetric and deviatoric strains in  $\hat{p} - \hat{q}$  space can be expressed as

$$\begin{Bmatrix} d\hat{p} + B_1 ds \\ d\hat{q} + B_2 ds \end{Bmatrix} = \begin{pmatrix} KA_1 & 3KGA_2 \\ 3KGA_2 & 3GA_3 \end{pmatrix} \begin{Bmatrix} d\varepsilon_v - d\varepsilon_{vs} \\ d\varepsilon_d \end{Bmatrix} \tag{38}$$

where

$$A_1 = T(M_{Ys}^4 - \hat{\eta}^4)\hat{p}A_0 + 12TGc_p\hat{\eta}^2 \tag{39}$$

$$A_2 = -2Tc_p(M^2 - \hat{\eta}^2)\hat{\eta} \tag{40}$$

$$A_3 = T[A_0(M_{Ys}^4 - \hat{\eta}^4)\hat{p} + Kc_p(M^2 - \hat{\eta}^2)^2] \tag{41}$$

$$B_1 = -T[A_0(M_{Ys}^4 - \hat{\eta}^4)\hat{p}k + 12Gc_p\hat{\eta}^2k] + TKc_p(M^2 - \hat{\eta}^2)\hat{p}f_s \tag{42}$$

$$B_2 = 6TGc_p\hat{\eta}[(M^2 + \hat{\eta}^2)\hat{p}f_s + k(M^2 - \hat{\eta}^2)] \tag{43}$$

$$T = \frac{1}{A_0(M_{Ys}^4 - \hat{\eta}^4)\hat{p} + 12Gc_p\hat{\eta}^2 + Kc_p(M^2 - \hat{\eta}^2)^2} \tag{44}$$

The proposed model can be further generalise to the three-dimensional (3D) stress space through the transformed stress (TS) method [33–35, 42], in which the irregular yield or failure surface based on the Matsuoka-Nakai criterion [20] can be converted to be circular in the deviatoric plane as shown in Fig. 4. The derivation process of the 3D stress–strain formulations is detailed in the Appendix. As shown by Eqs. (11) and (12), when the suction remains constant, the expansion potential becomes zero and the proposed model can reduce to the original UH model for unsaturated soils [41]. It is noted that the capacity of the proposed model in simulating true triaxial path with a constant suction have been fully verified in the previous studies [41] and, therefore, is not detailed in this paper.

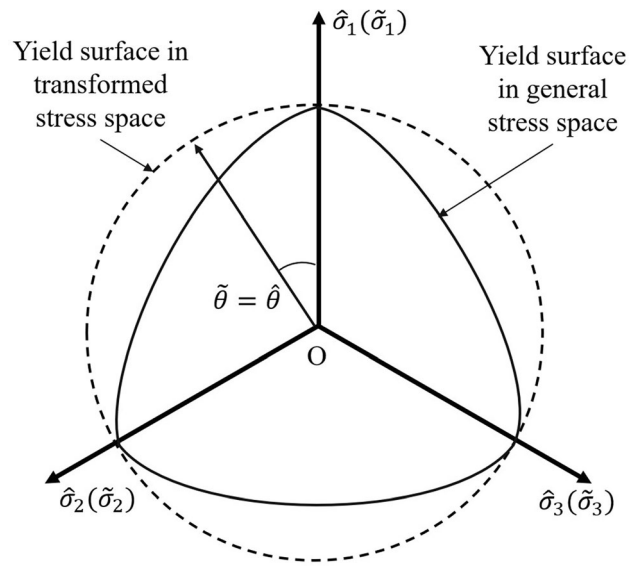


Fig. 4 Stress transformation from general stress space to transformed stress space

### 5 Fundamental features of the proposed model

There are eleven parameters required in the proposed UH model for unsaturated expansive clays:  $\kappa$ ,  $M$ ,  $\nu$ ,  $\lambda(0)$ ,  $\lambda_s$ ,  $\kappa_s$ ,  $p^c$ ,  $\gamma$ ,  $\beta$ ,  $k$  and  $J$ . The first ten parameters are the same as those defined in the BBM which can be determined based on results of the triaxial compression tests on unsaturated clays under different suctions and the drying-wetting cycle tests at a given net mean stress. The additional parameter  $J$  which demonstrates the expansion potential can be calibrated based on the results of wetting tests under different net mean stresses.

In this section, the capability of the proposed model in describing the swelling of unsaturated expansive clays

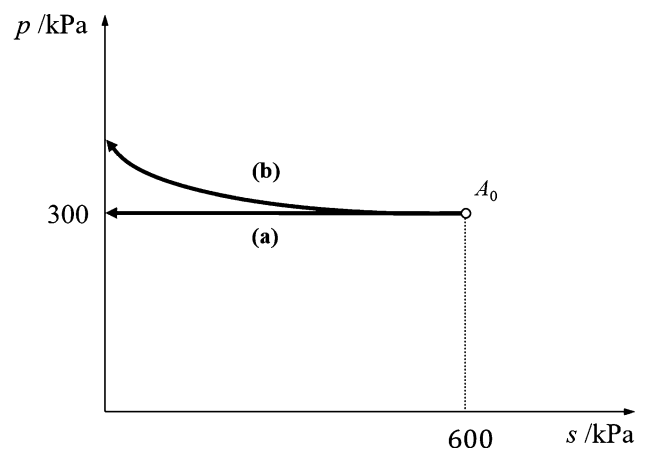


Fig. 5 Stress paths of wetting after isotropic compression and reloading



during wetting is demonstrated in the following simulations with the stress paths shown in Fig. 5 and the model parameters listed in Table 1.

In this simulation, the volumetric change of unsaturated clays is mainly related to three parameters: parameter,  $J$ , initial dry density,  $\rho_d$ , and the overconsolidation parameter,  $R_s$ , with the latter two showing the influence of degree of clay compaction on swelling behaviour. In this section, for simplicity, a constant ratio of  $\rho_d/\rho_w = 1.5$  is adopted and the effects of variation in both  $J$  and  $R_s$  have been investigated. In addition, as the overconsolidation parameter  $R_s$  varies with suction (see Eq. 14), OCR is adopted instead in the parametric study to demonstrate the effect of compaction status on the volumetric change during wetting. In this paper, the OCR is defined as the ratio of the pre-consolidation pressure to the current net mean stress.

### 5.1 Volume changes due to wetting

The influence of the values of  $J$  on the volumetric change is demonstrated in the simulation of the loading–unloading–wetting path. In this simulation, under the constant suction of  $s = 600$  kPa, the clay samples were isotropically compressed from the initial net mean stress of  $p = 300$  kPa to  $p = 1000$  kPa and then unloaded to  $p = 300$  kPa to achieve an OCR of 3.33. Then they were wetted to the saturation status under the constant pressure (i.e.  $p = 300$  kPa), as shown by path (a) in Fig. 5.

Figure 6 demonstrates the predicted volumetric strain of the clay samples during wetting with different values of  $J = 0, 2, \text{ and } 5$ . It can be seen that with the decrease of suction, expansive volume change of the clays occurs. When  $J = 0$ , the proposed model reduces to the UH model for unsaturated soils and there is no plastic expansion volumetric strain induced by the swelling of the microstructure,  $\epsilon_{vs}^p$ . Only the elastic volumetric strain induced by the suction decreasing,  $d\epsilon_{vs}^e$ , occurs, which leads to the slight volume expansion in Fig. 6. When  $J = 2$  and 5, volume change due to the swelling of the microstructure (i.e.  $\epsilon_{vs}^p$ ) occurs, which contributes to the expansive volume change of the clays. Moreover, increasing the values of  $J$  can lead to a significant increase of the expansive volume change. When the clay is reaching

**Table 1** Parameter values of simulation

Parameter	$\lambda(0)$	$\kappa$	$\lambda_s$	$\nu$	$M$	$k$
Value	0.2	0.02	0.08	0.3	1.0	0.01
Parameter	$r$	$\kappa_s$	$p^c$ (kPa)	$\beta$ (kPa) <sup>-1</sup>	$P_{at}$ (kPa)	$e_0$
Value	0.45	0.012	100	0.01	100	0.8

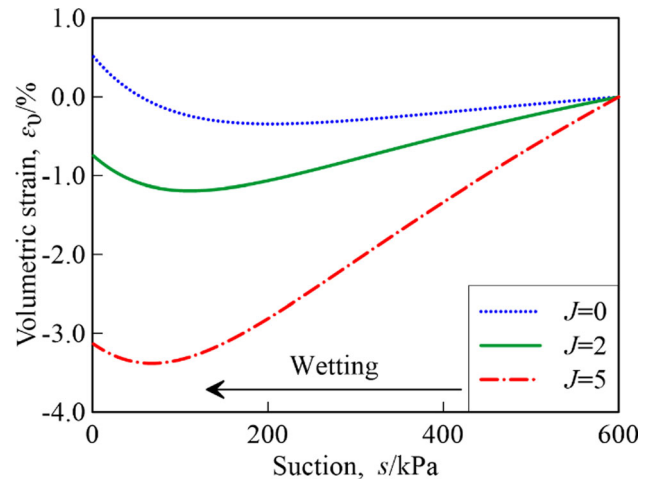


**Fig. 6** Volumetric strain during wetting with different values of  $J$

the saturated condition, a wetting-collapse feature can be observed. This is because when the suction is close to 0 kPa the current stress state of the clays is close to the yield surface and the size of the plastic volumetric strain induced by the reduction of suction,  $\epsilon_{vp}^p$ , exceeds the plastic expansion volumetric strain induced by the swelling of the microstructure,  $\epsilon_{vs}^p$ . As a result, the total volume change of the clays is dominated by the former compressive volume change.

The influence of different OCRs on the volumetric change is demonstrated following a similar manner. In the simulation, the initial horizontal and vertical stresses were set as 300 kPa, while initial suction was set as 600 kPa. The unsaturated clay samples were compressed isotropically to  $p = 500$  kPa, 1000 kPa, and 1500 kPa, and then unloaded to  $p = 300$  kPa to achieve the OCRs of 1.67, 3.33 and 5, respectively. Subsequently, the samples were wetted

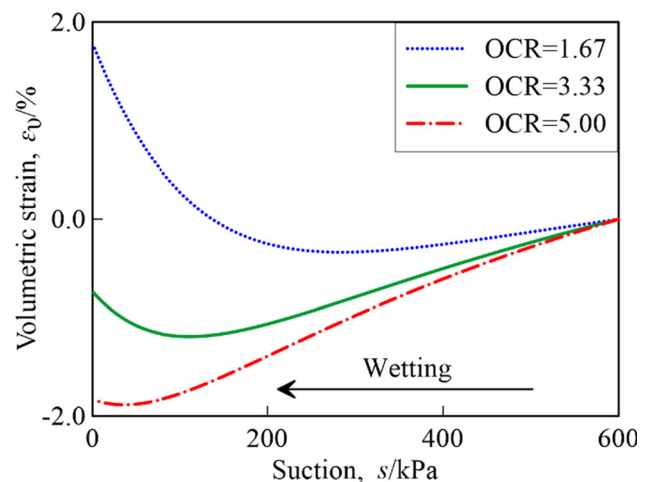


**Fig. 7** Volumetric strain during wetting with different values of OCR

to the saturation status under the constant pressure (i.e.  $p = 300$  kPa) with  $J = 2$ , as shown by path (a) in Fig. 5.

Figure 7 shows the predicted volumetric strain of the clay samples during wetting with different OCRs. It can be seen that at the beginning of wetting, all samples exhibited expansive volume change with decreasing suction, and a higher OCR can result in a larger volume increase. When the saturated condition is reaching, wetting-collapse can be observed which is also because that the size of the compressive plastic volumetric strain induced by the suction decrease,  $\varepsilon_{vp}^p$ , exceeds the expansive plastic volumetric strain induced by the swelling of the microstructure,  $\varepsilon_{vs}^p$ . It is noted that the simulation results are consistent with the observed features of volumetric change in the experimental tests of overconsolidated expansive soils by Wang et al. [30]

## 5.2 Swelling pressure

The swelling pressure is a basic variable for describing the swelling characteristics of unsaturated expansive clays, which can be measured through the following two testing methods [11]. The first approach is to make the clays wet and deform freely and then increase the pressure on the clays after wetting to reduce the volume of the clays until the initial volume before wetting is reached. The applied pressure is considered as the swelling pressure. In the second method, the volume of the clays remains unchanged by continuously adjusting the confining pressure during wetting, and the pressure increase is referred to as the swelling pressure. In this simulation, the second method is used to monitor the change of swelling pressure during wetting. Therefore, the following stress path of loading–unloading–wetting is adopted: The unsaturated clay samples are firstly compressed isotropically and unloaded under the constant suction, and are then wetted to saturation with increasing net mean stress which ensure a constant clay volume during wetting, as shown by the path (b) in Fig. 5. The swelling pressure is measured as the increase in the applied net mean stress during wetting.

Figures 8 and 9 demonstrate the influences of  $J$  and OCR on the swelling pressure change, respectively, in the simulation which adopts the same initial stress condition and loading–unloading process as that described in the previous section. A similar feature can be observed compared to that of the volumetric change during wetting. When  $J = 0$ , a slight increase of the swelling pressure occurs as only the elastic volumetric strain induced by the suction decreasing,  $d\varepsilon_{vs}^e$  exists. When  $J = 2$  and 5, the swelling of the microstructure results in an increase in the swelling pressure, and increasing values of  $J$  can lead to an increase of the maximum swelling pressure. When the

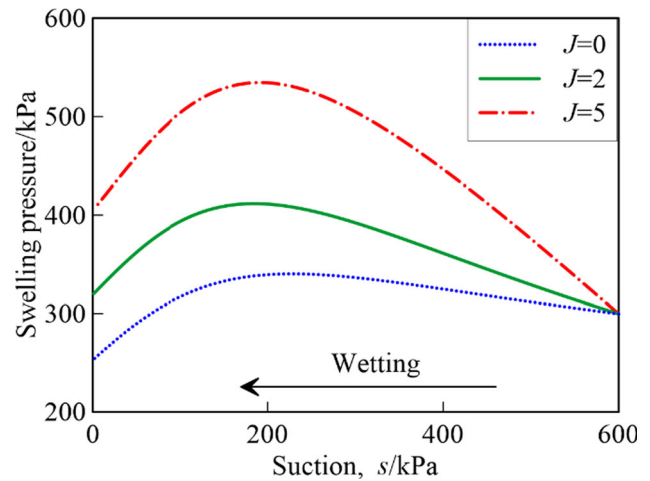


Fig. 8 Variation of swelling pressure during wetting under a constant volume with different values of  $J$

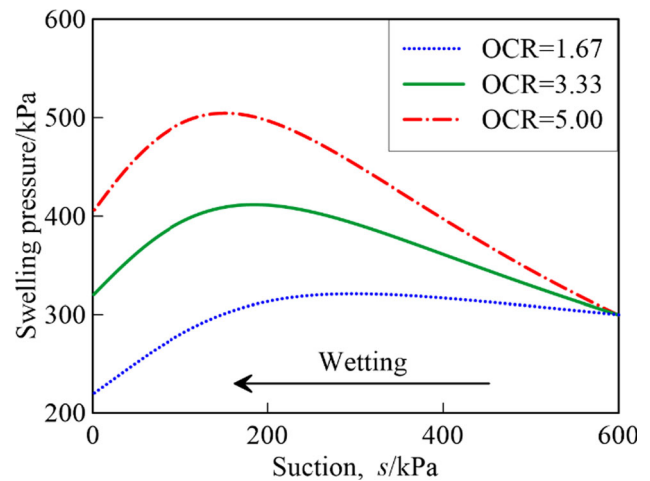


Fig. 9 Variation of swelling pressure during wetting under a constant volume with different values of OCR

saturated condition is reached, the clays tend to collapse and thus the swelling pressure decreases to maintain a constant sample volume. As shown in Fig. 9, with increasing OCR, the maximum swelling pressure of the clay samples also increases.

## 6 Test results and model predictions

In order to verify the capability of the proposed model, simulations of a series of existing relevant tests on unsaturated expansive clays from Zhan et al. [48], Alonso et al. [2] and Zhan [47] have been carried out in this paper. As shown by Eqs. (11) and (12), when the suction remains constant, the expansion potential becomes zero and the proposed model can reduce to the original UH model for unsaturated soils [41]. As stated by Gens and Alonso [9]

and Escario and Saez [7], the mechanical behaviour of expansive soils with constant suctions is similar to that of general unsaturated soils. Therefore it is believed that the capacity of the proposed model in simulating various stress paths with a constant suction have been fully verified in the previous study [41] and hence is not detailed in this paper.

### 6.1 Wetting tests on Zaoyang expansive clays

Zhan et al. [48] conducted indoor tests on the expansive clays from a slope in Zaoyang, Hubei province of China. The dry density of the clay samples was  $1.52\text{--}1.60 \times 10^3 \text{ kg/m}^3$ . The contents of sand, silts, and clays in the samples were reported as 3%, 58%, and 39%, respectively. The liquid limit of the clays was 50.5% and the plasticity index was 31%. The tests were carried out by employing the computer-controlled triaxial stress-path testing systems for unsaturated soils. Three sets of tests were considered in the simulation. In each test, the clay samples were prepared by static compaction with a maximum vertical compaction pressure of 800 kPa. After the suction balance, the suctions of the clay samples were controlled to be 200 kPa. Then with the suction unchanged, the samples were subjected to isotropic consolidation under the isotropic pressure of 40 kPa, 70 kPa and 100 kPa, respectively, resulting in a void ratio of 0.728, 0.726, and 0.723. After the consolidation was completed, the wetting test was performed in which the isotropic pressure was kept unchanged, while the suction was reduced from 200 to 0 kPa.

The model parameters adopted in the simulation which are determined based on existing studies [4, 13, 48] are listed in Table 2. In addition, the dry density of the clays before wetting was taken as  $1.56 \times 10^3 \text{ kg/m}^3$ , while the density of water was chosen as  $1.00 \times 10^3 \text{ kg/m}^3$ .

The comparison between the experimental results and the predicted results of the wetting process under different isotropic pressure are shown in Fig. 10. It can be seen that volume expansion occurs in the three groups of clay samples during wetting. A higher isotropic pressure can result in a lower volume expansion. The predicted curve is in good agreement with the experimental data, which demonstrates that the proposed model is capable of

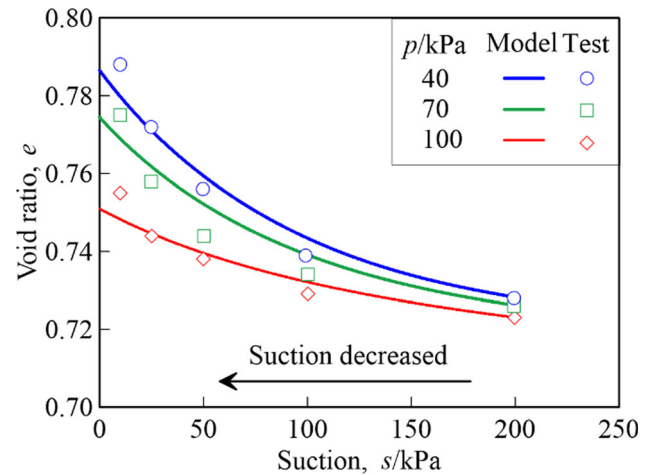


Fig. 10 Comparison in the variation of void ratio during wetting between test results by Zhan et al. [48] and model predictions

reproducing the process of volume expansion during wetting and the effect of isotropic pressure on the swelling behaviour.

### 6.2 Wetting tests on expansive Boom clays

Alonso et al. [2] conducted laboratory tests on expansive Boom clays which had a liquid limit of 55.9% and a plasticity index of 29.2%. The contents of kaolin, illite and montmorillonite in the clays were 20%, 30%, and 10%, respectively. Three sets of wetting tests under different vertical pressure were considered here. In all tests, the samples were first compacted under a vertical stress of approximately 2600 kPa, yielding a dry density of  $1.40 \times 10^3 \text{ kg/m}^3$ . The suctions of clay samples were controlled as 500 kPa, 500 kPa, and 700 kPa, respectively. Then the clay samples were consolidated under the vertical pressures of  $\sigma_v = 20 \text{ kPa}$ , 100 kPa, and 400 kPa, respectively, under the corresponding constant suction. After that, the wetting tests were performed with the suctions of the clay samples reducing to 0 kPa under a constant vertical pressure.

The parameters adopted in this simulation are listed in Table 3 and a ratio of  $\rho_d/\rho_w = 1.40$  was adopted.

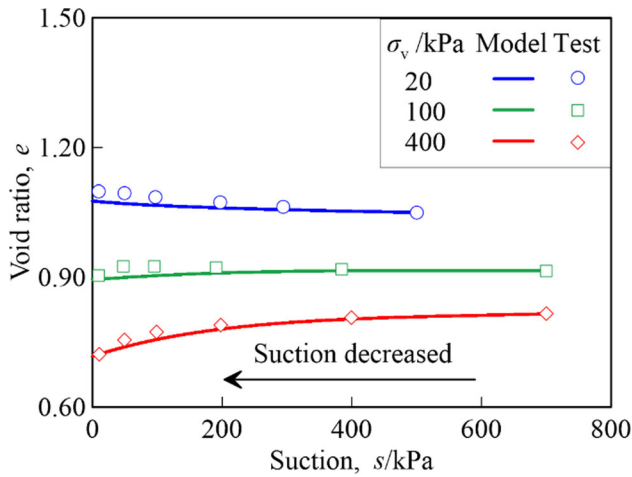
Figure 11 demonstrates the comparison between the experimental and predicted results. It can be seen that under different vertical pressures, the clay samples exhibit

Table 2 Model parameters for expansive clays from Zhan et al. [48]

Parameter	$\lambda(0)$	$\kappa$	$\lambda_s$	$\nu$	$M$	$k$
Value	0.1	0.01	0.1	0.3	1.0	0.01
Parameter	$r$	$\kappa_s$	$p^c \text{ (kPa)}$	$\beta \text{ (kPa)}^{-1}$	$P_{at} \text{ (kPa)}$	$J$
Value	0.095	0.018	100	0.025	100	2

Table 3 Model parameters for expansive clays from Alonso et al. [2]

Parameter	$\lambda(0)$	$\kappa$	$\lambda_s$	$\nu$	$M$	$k$
value	0.158	0.01	0.1	0.3	1.0	0.008
parameter	$r$	$\kappa_s$	$p^c \text{ (kPa)}$	$\beta \text{ (kPa)}^{-1}$	$P_{at} \text{ (kPa)}$	$J$
value	0.08	0.008	10	0.005	100	1.2



**Fig. 11** Comparison in the variation of void ratio during wetting between test results by Alonso et al. [2] and model predictions

different features of volume change during wetting. Under a low vertical pressure, the clay sample swells as its volume change is dominated by the plastic expansion volumetric strain induced by the swelling of the microstructure,  $\varepsilon_{vs}^p$ . When the vertical pressure increases, the LC yield surface is more likely to be activated during wetting, which will result in the collapsing of the sample. When the vertical pressure is sufficiently large, a compressive volume change of the sample can be observed. The predicted results by the proposed model can characterise such behaviour of expansive clays and are in a satisfactory agreement with the test results.

### 6.3 Wetting tests on silty expansive clays

A series of wetting tests on silty expansive clays were conducted by Zhan [47]. The tests were carried out by employing a suction-controlled double-cell triaxial apparatus for unsaturated clays and four sets of wetting tests were selected for model verification. The initial suctions of four groups of clay samples, RUT7, RUT8, RUT9, and RUT10, were controlled as 540 kPa and the isotropic pressures were kept unchanged at 20 kPa. Then clay samples were wetted to the suctions of 25 kPa, 50 kPa, 100 kPa, and 200 kPa, respectively. The model parameters

**Table 4** Model parameters for expansive clays from Zhan [47]

Parameter	$\lambda(0)$	$\kappa$	$\lambda_s$	$\nu$	$M$	$k$
Value	0.11	0.02	0.1	0.3	0.97	0.01
Parameter	$r$	$\kappa_s$	$p^c$ (kPa)	$\beta$ (kPa) <sup>-1</sup>	$P_{at}$ (kPa)	$J$
Value	0.3489	0.01	100	0.0294	100	2

in the simulation were determined based on existing studies [27, 47] which are listed in Table 4.

Figure 12 demonstrates the comparison in the variation of void ratio during wetting between the measured and predicted results, showing a good agreement.

## 7 Conclusions

To adequately describe the behaviour of unsaturated expansive clays, a novel expansion potential is firstly established in this paper which takes into account the effect of overconsolidation on the volume change of the microstructure during wetting. By introducing such parameter as well as an additional yielding mechanism for wetting, the UH model for unsaturated expansive clays is proposed. The characteristics of this model are summarised as follows:

(1) Based on the double-structure theory, a SD yield surface is introduced into the framework of the original UH model for unsaturated soils for modelling the volume change mechanism of unsaturated expansive clays during wetting.

(2) The effects of overconsolidation and stress path on the volumetric change of unsaturated expansive clays are taken into account by both the unified hardening parameter  $H$  and the proposed expansion potential in this paper. Moreover, the model is generalised to the 3D stress state by adopting the transformed stress method, without adding any new parameter.

(3) Only one additional parameter is introduced compared to the original UH model for unsaturated soils which can be determined based on the results of wetting tests under different net mean stresses. The predicted results by the proposed model show an excellent agreement against

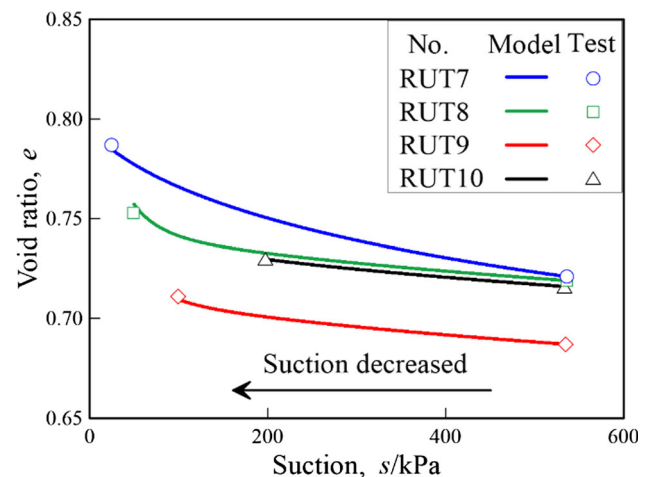


**Fig. 12** Comparison in the variation of void ratio during wetting between test results by Zhan [47] and model predictions

the experimental results from a series of existing studies, which verifies the capability of the proposed model in modelling the features of unsaturated expansive clays.

(4) It is noted that the couplings between the water retention curve (WRC) and the mechanical behaviour of unsaturated expansive clays, in particular the hysteresis behaviour of WRC during the cyclic wetting–drying process, are not taken into account in this study, and will be further investigated in the further work.

### Appendix: Derivation of three-dimensional elastoplastic stress–strain relationship

As shown in Fig. 4,  $\hat{\sigma}_i = \sigma_i + p_s$  is the principal stress considering the suction and  $\hat{\theta}$  is the corresponding Lode’s angle. The transformation from the general stress space to the transformed stress space can be expressed as

$$\begin{cases} \tilde{\sigma}_{ij} = \hat{\sigma}_{ij}, \hat{q} = 0 \\ \tilde{\sigma}_{ij} = \hat{p}\delta_{ij} + \frac{\hat{q}_c}{\hat{q}}(\hat{\sigma}_{ij} - \hat{p}\delta_{ij}), \hat{q} \neq 0 \end{cases} \quad (45)$$

where

$$\hat{p} = \frac{\hat{\sigma}_1 + \hat{\sigma}_2 + \hat{\sigma}_3}{3} \quad (46)$$

$$\hat{q} = \sqrt{\frac{1}{2}[(\hat{\sigma}_1 - \hat{\sigma}_2)^2 + (\hat{\sigma}_2 - \hat{\sigma}_3)^2 + (\hat{\sigma}_3 - \hat{\sigma}_1)^2]} \quad (47)$$

$$\hat{q}_c = \frac{2\hat{I}_1}{3\sqrt{\frac{\hat{I}_1\hat{I}_2 - \hat{I}_3}{\hat{I}_1\hat{I}_2 - 9\hat{I}_3} - 1}} \quad (48)$$

$$\hat{I}_1 = \hat{\sigma}_{ii} \quad (49)$$

$$\hat{I}_2 = \frac{1}{2}[(\hat{\sigma}_{ii})^2 - \hat{\sigma}_{rs}\hat{\sigma}_{sr}] \quad (50)$$

$$\hat{I}_3 = \frac{1}{3}\hat{\sigma}_{ij}\hat{\sigma}_{jk}\hat{\sigma}_{ki} - \frac{1}{2}\hat{\sigma}_{rs}\hat{\sigma}_{sr}\hat{\sigma}_{mm} + \frac{1}{6}(\hat{\sigma}_{mm})^3 \quad (51)$$

Integrating Eq. (45), the UH model for unsaturated expansive clays in 3D stress space can be expressed using tensor as

$$d\sigma_{ij} + d\sigma_{ij}^{p_s} = D_{ijkl}^{ep}(de_{kl} - de_{kl}^e - de_{kl}^{p_m}) \quad (52)$$

where  $\sigma_{ij}^{p_s}$  is the stress related to  $p_s$ ,  $e_{kl}^e$  is the elastic strain induced by  $p_s$ ,  $e_{kl}^{p_m}$  is the plastic strain induced by the microstructural swelling and  $D_{ijkl}^{ep}$  is the elasto-plastic constitutive tensor which can be expressed as:

$$D_{ijkl}^{ep} = L\delta_{ij}\delta_{kl} + G(\delta_{ik}\delta_{jl} + \delta_{il}\delta_{jk})\# \\ - \frac{(L\frac{\partial \tilde{f}}{\partial \tilde{\sigma}_{mm}}\delta_{ij} + 2G\frac{\partial \tilde{f}}{\partial \tilde{\sigma}_{ij}})(L\frac{\partial \tilde{f}}{\partial \tilde{\sigma}_{mm}}\delta_{kl} + 2G\frac{\partial \tilde{f}}{\partial \tilde{\sigma}_{kl}})}{X} \quad (53)$$

where

$$X = L\frac{\partial \tilde{f}}{\partial \tilde{\sigma}_{ii}}\frac{\partial \tilde{f}}{\partial \tilde{\sigma}_{kk}} + 2G\frac{\partial \tilde{f}}{\partial \tilde{\sigma}_{ij}}\frac{\partial \tilde{f}}{\partial \tilde{\sigma}_{ij}} - \frac{\partial \tilde{f}}{\partial p_x}\frac{\partial p_x}{\partial p_x^*}\frac{1}{\tilde{\Omega}} \quad (54)$$

$$L = K - \frac{2}{3}G \quad (55)$$

$\tilde{f}$  is the current yield surface in the transformed stress space which can be expressed as

$$\tilde{f} = \ln \tilde{p} + \ln\left(1 + \frac{\tilde{q}^2}{M^2\tilde{p}^2}\right) - \ln(p_x + p_s) = 0 \quad (56)$$

where

$$\tilde{p} = \hat{p} \quad (57)$$

$$\tilde{q} = \hat{q}_c \quad (58)$$

and

$$\frac{1}{\tilde{\Omega}} = \frac{\tilde{M}_{Ys}^4 - \tilde{\eta}^4}{M^4 - \tilde{\eta}^4} \quad (59)$$

$$\tilde{M}_{Ys} = 6\left[\sqrt{\frac{\lambda}{R_s}\left(1 + \frac{\lambda}{R_s}\right)} - \frac{\lambda}{R_s}\right] \quad (60)$$

where

$$\tilde{\eta} = \frac{\tilde{q}}{\tilde{p}} \quad (61)$$

$$\tilde{R}_s = \frac{\tilde{p}}{\tilde{\Omega}} \quad (62)$$

**Acknowledgements** This paper was supported by the National Natural Science Foundation of China (Grant Nos. 52238007, and 51979001) and the National Key Research and Development Plan of China (Grant No. 2018YFE0207100).

### Declarations

**Conflict of interest** The authors declare that they have no known competing financial interests or personal relationships that could have appeared to influence the work reported in this paper.

### References

- Alonso EE, Gens A, Josa A (1990) A constitutive model for partially saturated soils. *Géotechnique* 40(3):405–430. <https://doi.org/10.1680/geot.1990.40.3.405>
- Alonso EE, Lloret A, Gens A, Yang DQ (1995) Experimental behaviour of highly expansive double-structure clay. In: Proc 1st international conference on unsaturated soils 1: 11–6



3. Alonso EE, Vaunat J, Gens A (1999) Modelling the mechanical behaviour of expansive clays. *Eng Geol* 54(1–2):173–183. [https://doi.org/10.1016/S0013-7952\(99\)00079-4](https://doi.org/10.1016/S0013-7952(99)00079-4)
4. Chen R (2007) Experimental study and constitutive modelling of stress-dependent coupled hydraulic hysteresis and mechanical behaviour of an unsaturated soil. PhD thesis, The Hong Kong University of Science and Technology, China
5. Chiu CF, Ng CWW (2003) A state-dependent elastoplastic model for saturated and unsaturated soils. *Géotechnique* 53(9):809–829. <https://doi.org/10.1680/geot.2003.53.9.809>
6. Chu TY, Mou CH (1973) Volume change characteristics of expansive soils determined by controlled suction test. In: Proc 3rd international conference on expansive soils 1: 177–185
7. Escario V, Saez J (1986) The shear strength of partly saturated soils. *Géotechnique* 36(3):453–456. <https://doi.org/10.1680/geot.1986.36.3.453>
8. Gao Y, Li Z, Cui W, Sun DA, Yu HH (2023) Effect of initial void ratio on the tensile strength of unsaturated silty soils. *Acta Geotech* 18:3609–3622. <https://doi.org/10.1007/s11440-023-01800-z>
9. Gens A, Alonso EE (1992) A framework for the behaviour of unsaturated expansive clays. *Can Geotech* 29(6):1013–1032. <https://doi.org/10.1139/t92-120>
10. Kassiff G, Baker R, Ovadia Y (1973) Swell-pressure relationships at constant suction changes. In: Proc 3rd international conference on expansive soils 1: 201–208
11. Kayabali K, Demir S (2011) Measurement of swelling pressure: direct method versus indirect methods. *Can Geotech* 48(3):354–364
12. Kyokawa H (2021) A double structure model for hydro-mechano-chemical behavior of expansive soils based on the surface phenomena of mineral crystals. *Eng Geol* 294:106366. <https://doi.org/10.1016/j.enggeo.2021.106366>
13. Li J, Yin ZY, Cui YJ, Hicher PY (2017) Work input analysis for soils with double porosity and application to the hydro-mechanical modeling of unsaturated expansive clays. *Can Geotech* 54(2):173–187. <https://doi.org/10.1139/cgj-2015-0574>
14. Li W, Yang Q (2017) A macro-structural constitutive model for partially saturated expansive soils. *Bull Eng Geol Environ* 76(3):1075–1084. <https://doi.org/10.1007/s10064-016-0933-z>
15. Lloret A, Villar MV (2007) Advances on the knowledge of the thermo-hydro-mechanical behaviour of heavily compacted “FEBEX” bentonite. *Phys Chem Earth, Parts A/B/C* 32(8–14):701–715. <https://doi.org/10.1016/j.pce.2006.03.002>
16. Lloret-Cabot M, Wheeler SJ, Sánchez M (2017) A unified mechanical and retention model for saturated and unsaturated soil behavior. *Acta Geotech* 12:1–21. <https://doi.org/10.1007/s11440-016-0497-x>
17. Lu PH, Ye WM, He Y (2023) A constitutive model of compacted bentonite under coupled chemo-hydro-mechanical conditions based on the framework of the BExM. *Comput Geotech* 158:105360. <https://doi.org/10.1016/j.compgeo.2023.105360>
18. Lu ZH, Chen ZH, Sun SG (2002) Study on deformation and strength characteristic of expansive soil with triaxial tests. *CJRME* 21(5):717–723. <https://doi.org/10.3321/j.issn:1000-6915.2002.05.024>
19. Mašin D (2013) Double structure hydromechanical coupling formalism and a model for unsaturated expansive clays. *Eng Geol* 165:73–88. <https://doi.org/10.1016/j.enggeo.2013.05.026>
20. Matsuoka H, Nakai T (1974) Stress-deformation and strength characteristics of soil under three different principal stresses. *Proceed Japan Soc Civil Eng* 232:59–70. [https://doi.org/10.2208/jscej1969.1974.232\\_59](https://doi.org/10.2208/jscej1969.1974.232_59)
21. Ng CWW, Zhou C, Chiu CF (2020) Constitutive modelling of state-dependent behaviour of unsaturated soils: an overview. *Acta Geotech* 15:2705–2725. <https://doi.org/10.1007/s11440-020-01014-7>
22. Pousada PE (1982) Deformabilidad de arcillas expansivas bajo succión controlada. Doctoral thesis, Universidad Politécnica de Madrid, Spain.
23. Sánchez M, Gens A, do Nascimento Guimarães L, Olivella S, (2005) A double structure generalized plasticity model for expansive materials. *Int J Numer Anal Methods Geomech* 29(8):751–787. <https://doi.org/10.1002/nag.434>
24. Sheng DC (2011) Review of fundamental principles in modelling unsaturated soil behaviour. *Comput Geotech* 38(6):757–776. <https://doi.org/10.1016/j.compgeo.2011.05.002>
25. Sun DA, Matsuoka H, Yao YP, Ichihara W (2000) An elastoplastic model for unsaturated soil in three-dimensional stresses. *Soils Found* 40(3):17–28. [https://doi.org/10.3208/sandf.40.3\\_17](https://doi.org/10.3208/sandf.40.3_17)
26. Sun DA, Sheng DC (2005) An elastoplastic hydro-mechanical model for unsaturated compacted soils. In: Tarantino A, Romero E, Cui YJ editors. *Advanced experimental unsaturated soil mechanics* 249–55.
27. Sun WJ, Sun DA (2012) Coupled modelling of hydro-mechanical behaviour of unsaturated compacted expansive soils. *Int J Numer Anal Methods Geomech* 36(8):1002–1022. <https://doi.org/10.1002/nag.1036>
28. Wang Q, Cui YJ, Tang AM, Li XL, Ye WM (2014) Time- and density-dependent microstructure features of compacted bentonite. *Soils Found* 54(4):657–666. <https://doi.org/10.1016/j.sandf.2014.06.021>
29. Wang Q, Tang AM, Cui YJ, Barnichon JD, Ye WM (2013) Investigation of the hydro-mechanical behaviour of compacted bentonite/sand mixture based on the BExM model. *Comput Geotech* 54:46–52. <https://doi.org/10.1016/j.compgeo.2013.05.011>
30. Wang Y (2020) A thermo-hydro-mechanical coupled constitutive model for bentonite based on critical saturation state surface. PhD thesis, Tongji University, China
31. Wang Y, Ye WM, Wang Q, Chen YG, Cui YJ (2022) A critical saturated state-based constitutive model for volumetric behavior of compacted bentonite. *Can Geotech* 59(11):1872–1886. <https://doi.org/10.1139/cgj-2021-0213>
32. Wheeler SJ, Sivakumar V (1995) An elasto-plastic critical state framework for unsaturated soil. *Géotechnique* 45(1):35–53. <https://doi.org/10.1680/geot.1995.45.1.35>
33. Yao YP, Matsuoka H, Sun DA (1999) A unified elastoplastic model for clay and sand with the SMP criterion. In: Proc 8th Australia-New Zealand conference on geomechanics 2: 997–1003
34. Yao YP, Sun DA (2000) Application of Lade’s criterion to Cam-clay model. *J Eng Mech* 126(1):112–119. [https://doi.org/10.1061/\(ASCE\)0733-9399\(2000\)126:1\(112\)](https://doi.org/10.1061/(ASCE)0733-9399(2000)126:1(112))
35. Yao YP, Sun DA (2001) Closure of “application of Lade’s criterion to Cam-clay model.” *J Eng Mech* 127(6):632–633. [https://doi.org/10.1061/\(ASCE\)0733-9399\(2001\)127:6\(632\)](https://doi.org/10.1061/(ASCE)0733-9399(2001)127:6(632))
36. Yao YP, Hou W, Zhou AN (2009) UH model: three-dimensional unified hardening model for overconsolidated clays. *Géotechnique* 59(5):451–469
37. Yao YP, Yang YF, Niu L (2011) UH model considering temperature effects. *Sci China Technol Sci* 54(1):190–202. <https://doi.org/10.1007/s11431-010-4209-8>
38. Yao YP, Kong YX (2012) Extended UH model: three-dimensional unified hardening model for anisotropic clays. *J Eng Mech* 138(7):853–866. [https://doi.org/10.1061/\(ASCE\)EM.1943-7889.0000397](https://doi.org/10.1061/(ASCE)EM.1943-7889.0000397)
39. Yao YP, Gao ZW, Zhao JD, Wan Z (2012) Modified UH model: constitutive modeling of overconsolidated clays based on a parabolic Hvorslev envelope. *J Geotech Geoenviron Eng*

- 138(7):860–868. [https://doi.org/10.1061/\(ASCE\)GT.1943-5606.0000649](https://doi.org/10.1061/(ASCE)GT.1943-5606.0000649)
40. Yao YP, Zhou AN (2013) Non-isothermal unified hardening model: a thermos-elasto-plastic model for clays. *Geotechnique* 63(15):1328–1345
41. Yao YP, Niu L, Cui WJ (2014) Unified hardening (UH) model for overconsolidated unsaturated soils. *Can Geotech* 51(7):810–821. <https://doi.org/10.1139/cgj-2013-0183>
42. Yao YP, Wang ND (2014) Transformed stress method for generalizing soil constitutive models. *J Eng Mech* 140(3):614–629
43. Yao YP, Kong LM, Zhou AN, Yin JH (2015) Time-dependent unified hardening model: three-dimensional elastoviscoplastic constitutive model for clays. *J Eng Mech* 141(6):04014162-1–04014162-18
44. Yao YP, Tian Y, Gao ZW (2017) Anisotropic UH model for soils based on a simple transformed stress method. *Int J Numer Anal Methods Geomech* 41:54–78. <https://doi.org/10.1002/nag.2545>
45. Ye WM, Huang Y, Cui YJ, Tang YQ, Delage P (2005) Microstructural changing characteristics of densely compacted bentonite with suction under unconfined hydrating conditions. *CJRME* 24(24):4570–4575
46. Ye WM, Schanz T, Qian LX, Wang J, Arifin Y (2007) Characteristics of swelling pressure of densely compacted Gaomiaozhi bentonite GMZ01. *CJRME* 26(Suppl. 2):3861–3865
47. Zhan LT (2003) Field and laboratory study of an unsaturated expansive soil associated with rain-induced slope instability. PhD thesis, The Hong Kong University of Science and Technology, China
48. Zhan LT, Chen R, Ng CWW (2014) Wetting-induced softening behavior of an unsaturated expansive clay. *Landslides* 11(6):1051–1061
49. Zhou AN, Sheng DC (2015) An advanced hydro-mechanical constitutive model for unsaturated soils with different initial densities. *Comput Geotech* 63:46–66. <https://doi.org/10.1016/j.compgeo.2014.07.017>

**Publisher's Note** Springer Nature remains neutral with regard to jurisdictional claims in published maps and institutional affiliations.

Springer Nature or its licensor (e.g. a society or other partner) holds exclusive rights to this article under a publishing agreement with the author(s) or other rightsholder(s); author self-archiving of the accepted manuscript version of this article is solely governed by the terms of such publishing agreement and applicable law.